Magnetic Circular Dichroism Spectra of the Octahedral Niobium and Tantalum Subhalide Clusters $[M_6X_{12}]^{n+}$

By **D. J. Robbins** and **A. J. Thomson,*** School of Chemical Sciences, University of East Anglia, Norwich NOR 88C

The magnetic circular dichroism (m.c.d.) spectra of the octahedral niobium and tantalum subchloride clusters, $[M_6Cl_{12}]^{n+}$ (n = 2, 3, and 4) have been measured in solution at room temperature. The m.c.d. spectra provide for the first time an unambiguous assignment of the electronic spectra of the clusters within a LCAO bonding scheme. The assignment shows that all previous bonding schemes give rise to an incorrect ordering of one-electron levels. Spin-orbit coupling in these cluster systems is considered for the first time, and a revised bonding scheme is proposed on the basis of the new assignment. This is rationalised with the aid of a simple crystal-field model.

THE subhalides of niobium and tantalum $[M_6X_{12}]^{n+}$ [M = Nb or Ta; X = Cl or Br; n = 2, 3, or 4], contain a highly symmetrical cluster of metal atoms with internuclear distances close to those of the pure metal.[1] This has been taken as evidence for strong metal–metal binding and several bonding schemes attempting to describe this interaction have been reported.[2-4] The electronic spectra of the clusters are highly complex but an unambiguous assignment would provide a check on the success of theoretical descriptions of the metal–metal bonds. Since the complexes possess high symmetry, being octahedral, and are stable in solution, the technique of magnetic circular dichroism (m.c.d.) spectroscopy is ideally suited to aid in the assignment of their electronic spectra. This paper describes a study of the m.c.d. spectra of the subhalides. This leads to a clear assignment of their electronic spectra, which is not consistent with any of the bonding schemes so far suggested. An alternative scheme consistent with the new assignment has been derived in the course of this work.

The structure of the cluster $[M_6X_{12}]^{n+}$ is shown in Figure 1(a).[5] The shortest internuclear distance between the metal atoms in both $[Nb_6Cl_{12}]^{2+}$ and $[Ta_6Cl_{12}]^{2+}$ is *ca.* 2·9 Å which is almost exactly twice the atomic radii of 1·45 and 1·47 Å for niobium and tantalum.[6] In the complex $(M_6X_{12})^{n+}$ the formal oxidation state of each metal atom is $+2\frac{1}{3}$, $2\frac{1}{2}$, $2\frac{2}{3}$ as n = 2, 3, or 4, respectively. The possible oxidation states have been verified by redox

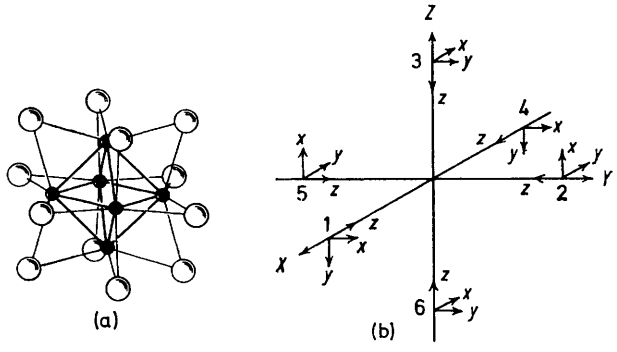

FIGURE 1 (a) The structure of the niobium and tantalum cluster, $[M_6X_{12}]^{n+}$. (b) The co-ordinate system and numbering of the metal atoms in an octahedral cluster [2]

[1] F. A. Cotton, *Quart. Rev.*, 1966, **20**, 389.
[2] F. A. Cotton and T. E. Haas, *Inorg. Chem.*, 1964, **3**, 10.
[3] M. B. Robin and N. A. Kuebler, *Inorg. Chem.*, 1965, **4**, 978.
[4] S. F. A. Kettle, *Theoret. Chim. Acta*, 1965, **3**, 211.
[5] P. A. Vaughan, J. H. Sturdivant, and L. Pauling, *J. Amer. Chem. Soc.*, 1950, **72**, 5477.
[6] I. M. Gibalo, 'Analytical Chemistry of Nb and Ta,' Ann Arbor, Humphrey Science Publishers, 1970.

titration,[7-9] by polarography,[8,10] and by spectroscopic and magnetic studies.[10,11] Conductance [10] and exchange measurements [7] indicate that the (M_6X_{12}) skeleton remains stable in solution, although ligands L may be attached to the metal atoms at terminal positions to form the species $(M_6X_{12})L_6$.[12]

X-Ray data on $K_4[(Nb_6Cl_{12})Cl_6]$,[13] $[Me_4N]_2[(Nb_6Cl_{12})Cl_6]$,[14] and $H_2[(Ta_6Cl_{12})Cl_6],nH_2O$ [15] show that the totally anated forms of both the niobium and the tantalum clusters have ideal octahedral symmetry. Previous work on the structure of $Ta_6Cl_{14},7H_2O$ [16] revealed a distorted polynucleus with two Ta atoms at the apices of an elongated tetragonal bipyramid.

It is evident that the distortion of the tantalum polyhedron in this case is brought about by the unsymmetrical nature of the apical ligands, 2 Cl^- and 4 H_2O, allied with hydrogen bonding between the water molecules in the lattice. On the other hand, in crystals of Nb_6Cl_{14} [17] no significant distortion ($\leqslant$0·06 Å) of the metal cluster is apparent. These results suggest that the tantalum cluster is more readily deformed than the niobium cluster. It is clear, however, that in solution the totally anated forms of both the niobium and tantalum clusters are perfectly octahedral. The electronic spectra (see below) reveal that the clusters remain undistorted in solution at least within the bandwidth of the absorption spectra, even when unsymmetrically solvated.[12]

There is evidence for extensive electron delocalisation over the octahedral skeleton of the cluster both from magnetic susceptibility measurements which show a very large diamagnetic term,[18] and from the e.p.r. spectrum of $(Nb_6Cl_{12})^{3+}$ which reveals hyperfine structure consistent with a single unpaired electron symmetrically delocalised over the six metal atoms.[10] The electronic spectra of the complexes reflect this delocalisation since transitions arise which are necessarily absent in the related mononuclear complexes. The most interesting of these are metal–metal transitions, that is, transitions between molecular orbitals derived principally from metal atomic orbitals. It is evident that these bands should be sensitive to the detailed mechanism of interaction between the metal atoms and that in addition their angular momentum, which may be derived from the m.c.d. spectra, should provide a good test of the suitability of any theoretical wavefunctions. The electronic spectra of the various oxidation states are unambiguously known, although many of the early magnetic and spectroscopic investigations are now known to be invalid because samples containing mixtures of oxidation states were used in the measurements. This aspect of the chemistry of these compounds has been fully reviewed by Hughes *et al.*[12] and Fleming and McCarley.[11]

The results of previous spectroscopic investigations may be summarised as follows.

(*a*) The bands below *ca.* 30,000 cm^{-1} in both Nb and Ta clusters show only small shifts when the bridging ligands are changed from Cl to Br, whereas the bands above 30,000 cm^{-1} show average shifts to lower energy of *ca.* 6000 cm^{-1}.[11] Therefore the lower-energy bands may be assigned to transitions between MO's derived principally from metal *d*-orbitals and the higher-energy bands to charge-transfer transitions.

(*b*) The changing of terminal ligands L has only a very small effect on both the metal–metal bands and on the charge-transfer bands.[11] This strongly suggests that charge transfer is from the bridging halogen atoms. It is of importance to notice that the number of metal–metal bands of a given metal polyhedron does not change. This bears out the evidence of the *X*-ray data in showing that the clusters remain undistorted even when unsymmetrically solvated.

(*c*) There is an almost perfect 1 : 1 correspondence of bands between analogous Nb and Ta complexes, the major discrepancy arising in the lowest-energy bands at *ca.* 10,000 cm^{-1}. There is also a 1 : 1 correspondence of bands at energies greater than *ca.* 15,000 cm^{-1} for the different oxidation states of each cluster, the lowest-energy bands showing the most marked changes with oxidation state.

(*d*) The similarities in the spectra of the clusters in different oxidation states indicate that there can be no gross re-ordering of energy levels following oxidation.

(*e*) The highest occupied orbital is spatially non-degenerate. This conclusion is based on e.p.r. data [10] and on magnetic susceptibility measurements which prove that the complex $(M_6X_{12})^{n+}$ is diamagnetic when $n = 2$ or 4, and paramagnetic with one unpaired electron when $n = 3$.[10,18] However it is also conceivable that the diamagnetism of the cluster $(M_6X_{12})^{4+}$ is the result of spin-orbit coupling within an orbitally-degenerate ground state. Since such ambiguity makes the assignment of the spectra difficult the possibility that spin-orbit coupling is important in determining the ground state of the complexes is discussed in Appendix A. There, however, it is shown to be inconsistent with the experimental data.

(*f*) Transitions between MO's belonging to a particular subsystem of atomic orbitals should be more intense than

[7] J. H. Espenson and R. E. McCarley, *J. Amer. Chem. Soc.*, 1966, **88**, 1063.
[8] R. E. McCarley, B. G. Hughes, F. A. Cotton, and R. Zimmerman, *Inorg. Chem.*, 1965, **4**, 1491.
[9] B. Spreckelmeyer and H. Schaefer, *J. Less-common Metals*, 1967, **13**, 127.
[10] R. A. Mackay and R. F. Schneider, *Inorg. Chem.*, 1967, **6**, 549.
[11] P. B. Fleming and R. E. McCarley, *Inorg. Chem.*, 1970, **9**, 1347.
[12] B. G. Hughes, J. L. Meyer, P. B. Fleming, and R. E. McCarley, *Inorg. Chem.*, 1970, **9**, 1343.
[13] A. Simon, H. G. von Schnering, H. Schafer, *Z. anorg. Chem.*, 1968, **361**, 235.
[14] F. W. Koknat and R. E. McCarley, referred to in ref. 12.
[15] R. A. Jacobson and C. B. Thaxton, *Inorg. Chem.*, 1971, **10**, 1460.
[16] R. D. Burbank, *Inorg. Chem.*, 1966, **5**, 1491.
[17] A. Simon, H. G. Schnering, H. Wöhrle, and H. Schäfer, *Z. anorg. Chem.*, 1965, **339**, 155.
[18] J. G. Converse and R. E. McCarley, *Inorg. Chem.*, 1970, **9**, 1361.

transitions between subsystems.[3,19] Configuration interaction may cause breakdown of this ' selection rule ' which should be applied with care.[11]

Molecular Orbital Calculation.—Three essentially different bonding schemes have been used for these cluster compounds. The first, and most widely quoted scheme, is that due to Cotton and Haas,[2] in which the molecular orbitals (MO's) involved in bonding within the M_6 octahedron are symmetry-adapted LCAO functions involving only metal *d*-orbitals. Slater 5*d*-orbitals were used in the calculation and all *d*-orbitals were considered degenerate in the absence of the metal–metal interaction. A second model, proposed by Robin and Kuebler [3] includes a contribution to the bonding MO's from both the metal *d*-orbitals and the halogen *p*-orbitals, the degeneracy of the *d*-orbitals on each metal being lifted by interaction with the bridging ligands. The order of the MO's predicted by this calculation is quite different from that given by Cotton and Haas. However, both schemes have several common features. The construction of MO's from symmetry adapted combinations of metal *d*-orbitals leads to ' subsystems ' of MO's derived from *d*-orbitals of a particular symmetry with respect to the localised metal atom coordinate sets, and in both schemes it is found that mixing between MO's of like symmetry belonging to different subsystems is small. Also off-diagonal matrix elements of the Hamiltonian are taken to be proportional to the overlap integral between the appropriate two atoms. A third model [4] describes the bonding in terms of topological equivalent orbitals. While this approach has useful qualitative value in emphasising similarities in the bonding of a wide range of cluster compounds it has not been used for quantitative calculations. In this work we seek an interpretation only of the *d*–*d* spectra of the cluster complexes, and when formulating a bonding scheme approach to these systems it is evident that three factors can play a major part in deciding the ordering of the *d* electron energy levels. These are: (i) the metal–metal interaction, (ii) the metal–ligand interaction, and (iii) spin-orbit coupling (since elements of large atomic number are involved).

The first of these is an unknown quantity, although it must be large since empirically the *d*–*d* spectra of these systems are unique to the polynuclear complex. With regard to the second it has been pointed out that the terminal ligands have only a small effect on the spectra, and for the present purpose it is reasonable to assume that the principal interaction is between a metal atom and the four nearest neighbour bridging ligands with which it forms a pseudo square-planar complex [see Figure 1(a)]. The magnitude of this splitting is unknown, although from the *d*–*d* spectra of hexachloro-complexes of Nb^{II} and Nb^{III} the octahedral crystal-field parameter *Dq* is found to be *ca.* 2300 and 2800 cm^{-1} respectively.[20] It is expected to be higher for the third-row transition-element tantalum. Thirdly the spin-orbit coupling parameters ζ_d for atomic niobium and tantalum are 475 and 1657 cm^{-1} respectively.[21a]

Thus in first order it seems clear that spin-orbit coupling will be small compared to the metal–ligand interaction, a conclusion supported by the close similarity between the spectra of corresponding Nb and Ta complexes for which spin-orbit coupling will be markedly different. However the effects of metal–metal and metal–ligand interaction may well be comparable in magnitude, and we feel that both should be included in any physically meaningful bonding scheme.

By analogy with the situation for square-planar complexes [22] it is clear from the co-ordinate system of Figure 1(b) that interaction between a metal atom and its four near-neighbour ligands will lift the degeneracy of the *d*-orbitals in the order:

$$d_{z^2} < d_{yz},\ d_{xz} < d_{xy} \ll d_{x^2-y^2} \qquad (1)$$

The *d*-orbitals on each metal atom therefore give rise to four sets, separated in energy by the local ligand field. The symmetry operations of the O_h point group (to which the complex as a whole belongs) transform each set into the corresponding set centred on a different metal atom. As a consequence of this symmetry-determined separability the orbitals belonging to a particular set on each of the six metal atoms may be combined to generate LCAO–MO's appropriate to the cluster complex. This last procedure gives rise to more-or-less independent subsystems of MO's derived from *d*-orbitals of a particular symmetry with respect to the local ligand field, and is essentially the procedure used by Cotton and Haas.[2] In this work we follow Cotton and Haas in assuming that only *d*-orbitals are important in the metal–metal bonding, and that as a result of the local ligand field the $d_{x^2-y^2}$ orbitals are too high in energy to play a significant part in this bonding. Hence, using the abbreviated notation for atomic *d*-orbitals given by Griffith,[21a] the MO's formed by combination of *d*-orbitals on the six metal atoms are found to transform in the following way in the O_h group:

$$\theta\ (\equiv d_{z^2}):\ a_{1g} + e_g + t_{1u}$$
$$\zeta\ (\equiv d_{xy}):\ a_{2u} + e_u + t_{2g}$$
$$\xi\eta\ (\equiv d_{yz}, d_{zx}):\ t_{1g} + t_{1u} + t_{2g} + t_{2u}$$

The basis functions for these irreducible representations have been derived to be consistent with the standard transformation relations for the O_h point group,[21b] and are given (not normalised) in Table 1.

We have repeated the calculation of Cotton and Haas since a check revealed that their results are in error; in addition their ordering of energy levels for the $|d_{z^2}|$ subsystem does not agree with that given by Robin and Kuebler, where agreement is expected on symmetry

[19] R. F. Schneider and R. A. Mackay, *J. Chem. Phys.*, 1968, **48**, 843.
[20] S. Basu, *J. Inorg. Nuclear Chem.*, 1966, **28**, 2769.
[21] (*a*) J. S. Griffith, ' The Theory of Transition Metal Ions,' Cambridge University Press, 1961; (*b*) *ibid.*, Table A16.
[22] P. Day, A. F. Orchard, A. J. Thomson, and R. J. P. Williams, *J. Chem. Phys.*, 1965, **42**, 1973.

TABLE 1

Basis functions * for the octahedral cluster complexes (un-normalised)

$|d_{xy}|$

a_{2u} : $(\zeta_1 + \zeta_2 + \zeta_3 - \zeta_4 - \zeta_5 - \zeta_6)$
e_u θ: $(-\zeta_1 + \zeta_2 + \zeta_4 - \zeta_5)$
ε: $(-\zeta_1 - \zeta_2 + 2\zeta_3 + \zeta_4 + \zeta_5 - 2\zeta_6)$
t_{2g} x: $(\zeta_1 + \zeta_4)$
y: $(\zeta_2 + \zeta_5)$
z: $(\zeta_3 + \zeta_6)$

$|d_{z^2}|$

a_{1g} : $(\theta_1 + \theta_2 + \theta_3 + \theta_4 + \theta_5 + \theta_6)$
e_g θ: $(-\theta_1 - \theta_2 + 2\theta_3 - \theta_4 - \theta_5 + 2\theta_6)$
ε: $(\theta_1 - \theta_2 + \theta_4 - \theta_5)$
t_{1u} x: $(\theta_1 - \theta_4)$
y: $(\theta_2 - \theta_5)$
z: $(\theta_3 - \theta_6)$

$|d_{yz},d_{xz}|$

t_{1g} x: $(\eta_2 - \xi_3 - \eta_5 + \xi_6)$
y: $(\xi_1 - \eta_3 - \xi_4 + \eta_6)$
z: $(\eta_1 + \xi_2 - \eta_4 - \xi_5)$
t_{1u} x: $-(\xi_2 + \eta_3 + \xi_5 + \eta_6)$
y: $(\eta_1 + \xi_3 + \eta_4 + \xi_6)$
z: $(-\xi_1 + \eta_2 - \xi_4 + \eta_5)$
t_{2g} x: $(\eta_2 + \xi_3 - \eta_5 - \xi_6)$
y: $(-\xi_1 - \eta_3 + \xi_4 + \eta_6)$
z: $(\eta_1 - \xi_2 - \eta_4 + \xi_5)$
t_{2u} x: $(-\xi_2 + \eta_3 - \xi_5 + \eta_6)$
y: $(-\eta_1 + \xi_3 - \eta_4 + \xi_6)$
z: $-(\xi_1 + \eta_2 + \xi_4 + \eta_5)$

* Functions obey standard transformation relations (ref. 21*b*).

grounds. In this Hückel-type calculation the MO energy is obtained from the relation:

$$\langle\psi_n|H|\psi_n\rangle = E_n\langle\psi_n|\psi_n\rangle \qquad (2)$$

where

$$\psi_n = \sum_{i=1}^{6} C_{ni}\phi_i$$

The integral $H_{ii} = \langle\phi_i|H|\phi_i\rangle$ is taken as the unit of energy, and as a first approximation is the same for all *d*-orbitals ϕ. Off-diagonal elements are obtained from the relation [2,3]

$$H_{ij} = 2S_{ij}H_{ii} \qquad (3)$$

where S_{ij} is the overlap integral $\langle\phi_i|\phi_j\rangle$.

Using these approximations the MO energies, in units of H_{ii}, are given by the following expressions. (It is implicit that overlap integrals refer to the atoms denoted by subscripts on left-hand side of the appropriate equations).

$|d_z|$ *Subsystem*

$$\begin{aligned} a_{1g} &\quad (1 + 8S_{12} + 2S_{14})/(1 + 4S_{12} + S_{14}) \\ e_g &\quad (1 - 4S_{12} + 2S_{14})/(1 - 2S_{12} + S_{14}) \\ t_{1u} &\quad (1 - 2S_{14})/(1 - S_{14}) \\ S_{12}(\theta,\theta) &= \tfrac{1}{16}S(d\sigma,d\sigma) + \tfrac{3}{4}S(d\pi,d\pi) + \tfrac{3}{16}S(d\delta,d\delta) \\ S_{14}(\theta,\theta) &= S(d\sigma,d\sigma) \end{aligned} \qquad (4)$$

$|d_{xy}|$ *Subsystem*

$$\begin{aligned} a_{2u} &\quad (1 + 8S_{12} - 2S_{14})/(1 + 4S_{12} - S_{14}) \\ e_u &\quad (1 - 4S_{12} - 2S_{14})/(1 - 2S_{12} - S_{14}) \\ t_{2g} &\quad (1 + 2S_{14})/(1 + S_{14}) \\ S_{12}(\zeta,\zeta) &= \tfrac{1}{2}[S(d\pi,d\pi) + S(d\delta,d\delta)] \\ S_{14}(\zeta,\zeta) &= S(d\delta,d\delta) \end{aligned} \qquad (5)$$

$|d_{yz},d_{xz}|$ *Subsystem*

$$\begin{aligned} t_{1g} &\quad (1 + 4S_{12}^{a} - 2S_{14})/(1 + 2S_{12}^{a} - S_{14}) \\ t_{2g} &\quad (1 - 4S_{12}^{a} - 2S_{14})/(1 - 2S_{12}^{a} - S_{14}) \\ t_{1u} &\quad (1 - 4S_{12}^{b} + 2S_{14})/(1 - 2S_{12}^{b} + S_{14}) \\ t_{2u} &\quad (1 + 4S_{12}^{b} + 2S_{14})/(1 + 2S_{12}^{b} + S_{14}) \\ S_{12}^{a} &= \langle\eta_1|\xi_2\rangle = -[\tfrac{3}{4}S(d\sigma,d\sigma) + \tfrac{1}{4}S(d\delta,d\delta)] \\ S_{12}^{b} &= \langle\xi_1|\eta_2\rangle = -\tfrac{1}{2}[S(d\pi,d\pi) + S(d\delta,d\delta)] \\ S_{14}(\xi,\xi) &= S(d\pi,d\pi) \end{aligned} \qquad (6)$$

The next stage of the calculation involves mixing of MO's of like symmetry belonging to different subsystems. However consideration of local AO symmetry shows that this second-order interaction depends only upon two-centre integrals, and in practice it is found to be small.[3] In addition the subsystems of MO's arising from the *d*-orbitals differ in energy on the diagonal by an unknown amount as a consequence of the metal–ligand interaction, and for these reasons we neglect this second-order mixing in the calculation entirely. It does, however, constitute an extra parameter which should be borne in mind when fitting the experimental results to the theoretical model.

With this approximation the *d*-orbital subsystems are independent, and it is now possible to include the metal–ligand interaction in the calculation in first order simply by lifting the degeneracy of the origins of the *d*-orbital subsystems as shown in equation (1). The relative energy separations are arbitrary, but by considering as major parameters only the metal–ligand interaction and the *d*-orbital valence-state ionisation potential H_{ii} it is possible to arrive at an ordering of MO's for the cluster complex which is consistent with the experimental data. Spin-orbit coupling may then be included in the scheme as a final perturbation, and is considered separately in a later section.

The evaluation of the MO energies requires the assumption of wavefunctions for the metal *d*-orbitals. In view of the approximations already inherent in the calculation we follow Cotton and Haas and use simple Slater 5*d*-orbitals. This keeps the calculation manageable, and has the great advantage of making possible the separate evaluation of the various contributions to the orbital magnetic moment; in this way the relative importance of different terms can be most easily appreciated. In addition the large internuclear distance of *ca.* 3 Å between the metal atoms makes it more likely that the Slater orbitals are a reasonable approximation to the true wavefunctions in the region of large overlap. Finally, the MO energies and angular momenta are evaluated for various values of the Slater orbital exponent α, and where the calculated quantities are not over-sensitive to this parameter it seems improbable that the use of these wavefunctions can be a limiting factor in the model. This applies particularly when only the signs, rather than the magnitudes, of orbital angular momentum matrix elements are being considered. However the use of 5*d* orbitals restricts the calculation to the tantalum cluster; Slater 4*d* orbitals include a non-integral power of the radial function r with the

result that overlap integrals cannot be evaluated by the standard method.[23] The necessary overlap integrals were then obtained from tables.[24,25]

On this basis the energy-level diagrams of Figure 2 are obtained. Each subsystem is shown separately, and although the ordering of the energy zeros is $d_{z^2} < d_{yz}$, $d_{zx} < d_{xy}$ the relative displacements are not implied; in the Cotton and Haas limit the three diagrams would be reduced to one, with a common zero of energy. Since all metal atoms are equivalent and the cluster has regular 0_h symmetry the overlap integrals and hence the MO energies are functions of the single parameter ρ (= αR, where α is the orbital exponent and R the shortest metal–metal distance). Cotton and Haas [2] show that the physically reasonable values of ρ fall in the range 6—11. Finally the 16 metal valence

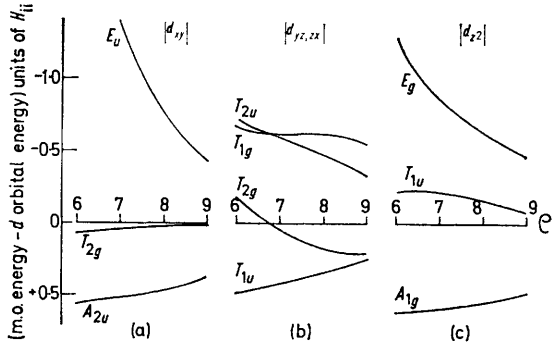

FIGURE 2 Energy-level diagrams for the cluster $(Ta_6Cl_{12})^{2+}$. Each d-orbital subsystem is shown separately. $\rho = \alpha R$, where α is the Slater orbital exponent and R is the shortest metal–metal distance

electrons of the complex $(M_6X_{12})^{2+}$ are considered to occupy the lowest energy MO's.

Calculation of M.c.d. Parameters.—In the m.c.d. spectrum the observed rotational strength for a transition is generally expressed as molar ellipticity per unit magnetic field parallel to the direction of propagation of the light beam. With the formalism first used by Buckingham and Stephens [26,27] we have

$$[\theta]_M = -21{\cdot}3458[f_1(B + C/kT) + f_2A] \quad (7)$$

where f_1 and f_2 are line-shape functions and the parameters A, B, C may be defined in terms of molecular quantities. Briefly one finds that a transition from a non-degenerate ground state to a degenerate excited state may be characterised by a non-zero value for the parameter A, whereas the occurrence of degeneracy in the ground state may produce a non-zero value for the parameter C. The signs and magnitudes of these parameters depend upon both the symmetries and the wavefunctions of the states involved in the transition.

The ground state of the cluster $(M_6X_{12})^{2+}$ is $^1A_{1g}$, and in this work we consider only electric-dipole allowed transitions $^1A_{1g} \longrightarrow {}^1T_{1u}$. Hence A terms may be associated with these transitions. On oxidation to $(M_6X_{12})^{3+}$ degeneracy is introduced into the ground state and C terms may be present in the m.c.d. spectrum. In this section we consider A terms for the species $(M_6X_{12})^{2+}$, and by this means are able to assign several bands in the spectrum. In a later section we use the proposed assignment to predict C terms for the species $(M_6X_{12})^{3+}$, a process which provides an independent check on the validity of the assignment.

Using the theoretical formalism given by Griffith [28] we have:

$$A(^1A_{1g} \longrightarrow {}^1T_{1u}) = \frac{i}{\sqrt{6}}\mu|m|^2 \quad (8)$$

where

$$\mu = \langle T_{1u}||\hat{\mu}||T_{1u}\rangle$$
$$m = \langle A_{1g}||\hat{m}||T_{1u}\rangle$$

and $\hat{\mu}$ and $\hat{m}$ are the magnetic and electric dipole moment operators respectively. The dipole strength of the transition is given by $D(^1A_{1g} \longrightarrow {}^1T_{1u}) = |m|^2$. The reduced matrix element μ may be expressed in terms of one-electron functions by using a standard method.[28] For an orbital excitation $a \rightarrow j$ we have

$$\mu(a \rightarrow j) = (-1)^{a+j} \cdot 3 \cdot \left[W\begin{pmatrix} a & a & T_1 \\ T_1 & T_1 & j \end{pmatrix}\langle a||\hat{\mu}||a\rangle + W\begin{pmatrix} j & j & T_1 \\ T_1 & T_1 & a \end{pmatrix}\langle j||\hat{\mu}||j\rangle \right] \quad (9)$$

where the W coefficients are tabulated by Griffith.[28]

From the results of the previous section we assume that those MO's derived from the d-orbitals which can be occupied in the ground state may only have the following symmetries: a_{1g}, a_{2u}, t_{1u}, t_{2g}. Table 2 then gives the magnetic moment matrix elements in the form of one-electron functions for all possible one-electron transitions involving the d-orbitals. The expressions have been simplified by using the fact that only T_1 and T_2 representations in the group 0_h have non-zero angular momentum. These one-electron reduced matrix elements must now be evaluated for the MO's of Table 1,

TABLE 2

The magnetic moment matrix elements expressed as one-electron functions (ref. 28)

One-electron transition	μ
$a_{1g} \rightarrow t_{1u}$	$+\langle t_{1u}\|\|\mu\|\|t_{1u}\rangle$
$a_{2u} \rightarrow t_{2g}$	$+\langle t_{2g}\|\|\mu\|\|t_{2g}\rangle$
$t_{2g} \rightarrow t_{2u}$	$\frac{1}{2}(\langle t_{2g}\|\|\mu\|\|t_{2g}\rangle + \langle t_{2u}\|\|\mu\|\|t_{2u}\rangle)$
$t_{1u} \rightarrow t_{1g}$	$\frac{1}{2}(\langle t_{1u}\|\|\mu\|\|t_{1u}\rangle + \langle t_{1g}\|\|\mu\|\|t_{1g}\rangle)$
$t_{2g} \rightarrow t_{1u}$	$-\frac{1}{2}(\langle t_{2g}\|\|\mu\|\|t_{2g}\rangle + \langle t_{1u}\|\|\mu\|\|t_{1u}\rangle)$
$t_{1u} \rightarrow t_{2g}$	$-\frac{1}{2}(\langle t_{1u}\|\|\mu\|\|t_{1u}\rangle + \langle t_{2g}\|\|\mu\|\|t_{2g}\rangle)$
$t_{2g} \rightarrow e_u$	$-\frac{1}{2}\langle t_{2g}\|\|\mu\|\|t_{2g}\rangle$
$t_{1u} \rightarrow e_g$	$-\frac{1}{2}\langle t_{1u}\|\|\mu\|\|t_{1u}\rangle$

and it is necessary to proceed in several stages: [29,30] (1) expand the matrix element in terms of the atomic orbitals; (2) make the co-ordinates of operator and

[23] R. S. Mulliken, C. A. Rieke, D. Orloff, and H. Orloff, *J. Chem. Phys.*, 1949, **17**, 1248.
[24] H. H. Jaffé, *J. Chem. Phys.*, 1953, **21**, 258.
[25] J. L. Roberts and H. H. Jaffé, *J. Chem. Phys.*, 1957, **27**, 883.
[26] A. D. Buckingham and P. J. Stephens, *Ann. Rev. Phys. Chem.*, 1966, **17**, 399.
[27] P. N. Schatz and A. J. McCaffery, *Quart. Rev.*, 1969, **23**, 552.
[28] J. S. Griffith, 'The Irreducible Tensor Method for Molecular Symmetry Groups,' Prentice-Hall Inc., New York, 1962.
[29] M. Gerloch and J. R. Miller, *Progr. Inorg. Chem.*, 1968, **10**, 1.
[30] D. J. Robbins, Ph.D. Thesis, University of East Anglia, 1971.

functions compatible; (3) simplify the resulting matrix elements using the Hermitian property of the operator; (4) obtain values for overlap integrals from tables, and evaluate numerically all other integrals. As a specific example consider the t_{2g} orbital derived from the $|d_{xy}|$ subsystem:

$$\langle t_{2g}||\hat{\mu}||t_{2g}\rangle = \frac{-\sqrt{6}}{N}\cdot\langle t_{2g}x|\hat{\mu}_z|t_{2g}y\rangle \qquad (10)$$
$$= \frac{-\sqrt{6}}{N}\cdot\langle\zeta_1+\zeta_4|\hat{\mu}_z|\zeta_2+\zeta_5\rangle$$

where N is a normalisation factor. Consider the term $\langle\zeta_1|\hat{\mu}_z|\zeta_2\rangle$. Only orbital angular momentum is significant in the singlet excited state, but it is defined with respect to the principal co-ordinate system of the complex, which we designate (0). It may be transformed to the co-ordinate system of metal atom (2) [Figure 1(b)]

$$\hat{L}_z^{(0)} = \hat{L}_x^{(2)} - i\hbar a\frac{d}{dy_2} \qquad (11)$$

where a is the distance from the centre of the complex to atom (2). Hence

$$\langle\zeta_1|\hat{\mu}_z|\zeta_2\rangle = -\beta\left\langle\zeta_1\left|\hat{L}_x^{(2)} - i\hbar a\frac{d}{dy_2}\right|\zeta_2\right\rangle \qquad (12)$$
$$= -i\hbar\beta\langle\zeta_1|\eta_2\rangle + i\hbar\beta a\left\langle\zeta_1\left|\frac{d}{dy_2}\right|\zeta_2\right\rangle$$

Using a simple transformation the function $\langle\zeta_1|\eta_2\rangle$ may be given in terms of standard overlap integrals. This procedure then gives the results below

$|d_{xy}|$ Subsystem

$$\langle t_{2g}x|\hat{\mu}_z|t_{2g}y\rangle = \frac{i}{N_\zeta(t_{2g})}\hbar\beta\left(2S(c)+4a\left\langle\zeta_1\left|\frac{d}{dy_2}\right|\zeta_2\right\rangle\right) \qquad (13)$$

$|d_{z^2}|$ Subsystem

$$\langle t_{1u}x|\hat{\mu}_z|t_{1u}y\rangle = \frac{i}{N_\theta(t_{1u})}\hbar\beta\left(\frac{3}{2}S(e)+4a\left\langle\theta_1\left|\frac{d}{dy_2}\right|\theta_2\right\rangle\right) \qquad (14)$$

$|d_{yz}, d_z|$ Subsystem

$$\langle t_{1g}x|\hat{\mu}_z|t_{1g}y\rangle = \frac{i}{N_{\xi\eta}(t_{1g})}\hbar\beta\left(2-8S(a)-2S(b)-2S(c)-4a\left\langle\xi_1\left|\frac{d}{dy_2}\right|\eta_2\right\rangle\right) \qquad (15)$$

$$\langle t_{2g}x|\hat{\mu}_z|t_{2g}y\rangle = \frac{i}{N_{\xi\eta}(t_{2g})}\hbar\beta\left(-2-8S(a)+2S(b)+2S(c)+4a\left\langle\xi_1\left|\frac{d}{dy_2}\right|\eta_2\right\rangle\right) \qquad (16)$$

$$\langle t_{1u}x|\hat{\mu}_z|t_{1u}y\rangle = \frac{i}{N_{\xi\eta}(t_{1u})}\hbar\beta\left(2+4S(d)+2S(b)+4a\left\langle\eta_1\left|\frac{d}{dy_2}\right|\xi_2\right\rangle\right) \qquad (17)$$

$$\langle t_{2u}x|\hat{\mu}_z|t_{2u}y\rangle = \frac{i}{N_{\xi\eta}(t_{2u})}\hbar\beta\left(-2+4S(d)-2S(b)-4a\left\langle\eta_1\left|\frac{d}{dy_2}\right|\xi_2\right\rangle\right) \qquad (18)$$

where
$$S(a) = [\tfrac{3}{4}S_{12}(d\sigma, d\sigma) + \tfrac{1}{4}S_{12}(d\delta, d\delta)]$$
$$S(b) = S_{14}(d\pi, d\pi)$$
$$S(c) = [S_{12}(d\pi, d\pi) - S_{12}(d\delta, d\delta)]$$
$$S(d) = [S_{12}(d\pi, d\pi) + S_{12}(d\delta, d\delta)]$$
$$S(e) = [S_{12}(d\delta, d\delta) - S_{12}(d\sigma, d\sigma)] \qquad (19)$$

and the normalisation factors may be obtained from equations (4)—(6).

Using Slater 5*d*-orbitals the overlap integrals may be obtained from tables,[24,25] but matrix elements of the type $\left\langle\phi\left|\frac{d}{dy}\right|\phi'\right\rangle$ must be evaluated numerically. It has been usual to neglect such terms because of the difficulty in their calculation, but their relative magnitude is of considerable interest in the present context and the necessary values have been calculated and tabulated.[30] With these results and an internuclear distance R of 2·9 Å obtained from *X*-ray data,[2] substitution in equations (13)—(18) gives Table 3. The magnetic

TABLE 3

The orbital magnetic moment *

$|d_{xy}|$ Subsystem.

ρ =	5	6	7	8
$2S(c)$	0·076	0·330	0·406	0·416
$4a\left\langle\zeta_1\left\|\frac{d}{dy_2}\right\|\zeta_2\right\rangle$	0·004	0·482	0·834	0·991
$\langle t_{2g}x\|\mu_z\|t_{2g}y\rangle$	+0·03	+0·38	+0·60	+0·69

$|d_{z^2}|$ Subsystem.

ρ =	5	6	7	8
$3/2S(e)$	0·686	0·406	0·127	−0·075
$4a\left\langle\theta_1\left\|\frac{d}{dy_2}\right\|\theta_2\right\rangle$	−0·781	−0·073	0·558	0·985
$\langle t_{1u}x\|\mu_z\|t_{1u}y\rangle$	−0·05	+0·21	+0·42	+0·53

$|d_{yz}, d_{xz}|$ Subsystem.

ρ =	5	6	7	8
$(a)t_{1g}$	2	2	2	2
$-8S(a)$	−0·343	−0·479	−0·852	−1·150
$-2S(b)$	−0·746	−0·554	−0·338	−0·200
$-2S(c)$	+0·164	−0·330	−0·406	−0·416
$-4a\left\langle\xi_1\left\|\frac{d}{dy_2}\right\|\eta_2\right\rangle$	+0·007	+0·481	+0·831	+0·991
$\langle t_{1g}x\|\mu_z\|t_{1g}y\rangle$	+0·50	+0·78	+0·50	+0·51
ρ =	5	6	7	8
$(b)t_{2g}$	−2	−2	−2	−2
$-8S(a)$	−0·343	−0·479	−0·852	−1·15
$+2S(b)$	+0·746	+0·554	+0·338	+0·200
$+2S(c)$	−0·164	+0·330	+0·406	+0·416
$+4a\left\langle\xi_1\left\|\frac{d}{dy_2}\right\|\eta_2\right\rangle$	−0·007	−0·481	−0·831	−0·991
$\langle t_{2g}x\|\mu_z\|t_{2g}y\rangle$	−0·62	−0·62	−0·70	−0·74
$(c)t_{1u}$	2	2	2	2
$+4S(d)$	2·760	2·764	2·172	1·680
$+2S(b)$	0·746	0·554	0·338	0·200
$+4a\left\langle\eta_1\left\|\frac{d}{dy_2}\right\|\xi_2\right\rangle$	−0·167	0·487	0·648	0·391
$\langle t_{1u}x\|\mu_z\|t_{1u}y\rangle$	+0·65	+0·74	+0·75	+0·70
$(d)t_{2u}$	−2	−2	−2	−2
$+4S(d)$	2·760	2·764	2·172	1·680
$-2S(b)$	−0·746	−0·554	−0·338	−0·200
$-4a\left\langle\eta_1\left\|\frac{d}{dy_2}\right\|\xi_2\right\rangle$	0·167	−0·487	−0·648	−0·391
$\langle t_{2u}x\|\mu_z\|t_{2u}y\rangle$	+0·07	−0·12	−0·32	−0·34

* Units of $i\hbar\beta$.

For notation see equation (19).

moment matrix elements are tabulated as a function of the parameter ρ, and the various contributions to the total magnetic moment are shown separately for comparison. It should be noted that terms of the type $a\left\langle \phi \left| \frac{d}{dy} \right| \phi' \right\rangle$ can make an appreciable contribution to the total magnetic moment and should not be dismissed as negligible.

The predicted A terms for possible one-electron transitions are obtained from equation (8) using Tables 2 and 3, and are given in Table 4 for various values of the parameter ρ. From Table 4 it is evident that the

TABLE 4

Predicted A/D values for the tantalum cluster complexes $(Ta_6X_{12})^{2+}$: (d-orbital subsystem in parentheses)

Transition	ρ = 6	7	8
* $a_{1g}(\theta) \rightarrow t_{1u}(\theta)$	+0·21	+0·42	+0·52
$a_{1g}(\theta) \rightarrow t_{1u}(\xi,\eta)$	+0·74	+0·75	+0·70
* $a_{2u}(\zeta) \rightarrow t_{2g}(\zeta)$	+0·38	+0·60	+0·69
$a_{2u}(\zeta) \rightarrow t_{2g}(\xi,\eta)$	−0·62	−0·70	−0·74
* $t_{1u}(\xi,\eta) \rightarrow t_{1g}(\xi,\eta)$	+0·76	+0·63	+0·61
* $t_{1u}(\xi,\eta) \rightarrow t_{2g}(\xi,\eta)$	−0·06	−0·03	+0·02
$t_{1u}(\xi,\eta) \rightarrow t_{2g}(\zeta)$	−0·56	−0·68	−0·70
$t_{1u}(\theta) \rightarrow t_{1g}(\xi,\eta)$	+0·50	+0·46	+0·52
$t_{1u}(\theta) \rightarrow t_{2g}(\xi,\eta)$	+0·21	+0·14	+0·11
$t_{1u}(\theta) \rightarrow t_{2g}(\zeta)$	−0·30	−0·51	−0·61
$t_{2g}(\xi,\eta) \rightarrow t_{1u}(\theta)$	+0·21	+0·14	+0·11
* $t_{2g}(\xi,\eta) \rightarrow t_{2u}(\xi,\eta)$	−0·37	−0·51	−0·54
* $t_{1u}(\theta) \rightarrow e_g(\theta)$	−0·11	−0·21	−0·26
$t_{1u}(\xi,\eta) \rightarrow e_g(\theta)$	−0·37	−0·38	−0·35

* Indicates intra-subsystem transition.

signs of the calculated A terms are constant over a range of values for ρ, although their magnitudes may change markedly. The one exception is the transition $t_{1u}(\xi,\eta) \longrightarrow t_{2g}(\xi,\eta)$. Therefore in the light of the earlier discussion it is possible to have some confidence in arguments based solely on the signs of the A terms.

Experimental Results.—Figures 3—6 give the absorption and m.c.d. spectra of $(Nb_6Cl_{12})^{n+}$ ($n = 2, 3, 4$) and of $(Ta_6Cl_{12})^{2+}$; Figure 7 gives the absorption spectra of

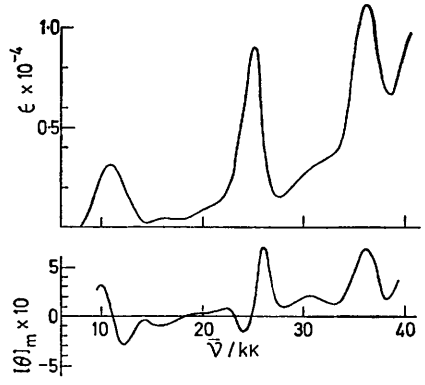

FIGURE 3 The absorption (upper curve) and m.c.d. (lower curve) spectra of $[Nb_6Cl_{12}]^{2+}$ in EtOH

$(Ta_6Cl_{12})^{n+}$ ($n = 3$ or 4) and Figure 8 compares the absorption spectra of $(Ta_6Cl_{12})^{2+}$ and $(Ta_6Br_{12})^{2+}$. For comparative purposes the absorption and m.c.d. spectra of the lowest-energy transitions of niobium and tantalum clusters in all three oxidation states are given in Figures 9 and 10.

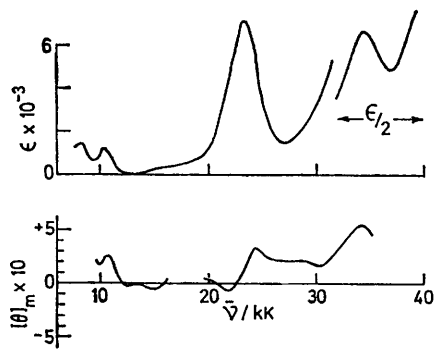

FIGURE 4 The absorption (upper curve) and m.c.d. (lower curve) spectra of $[Nb_6Cl_{12}]^{3+}$ in EtOH–HCl

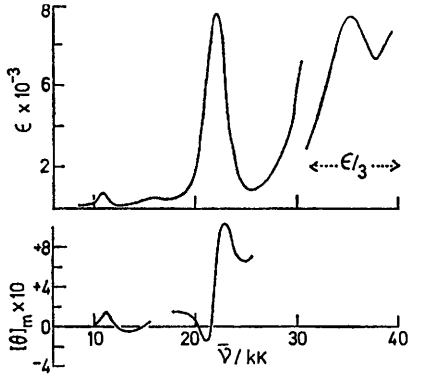

FIGURE 5 The absorption (upper curve) and m.c.d. (lower curve) spectra of $[Nb_6Cl_{12}]^{4+}$ in EtOH–HCl

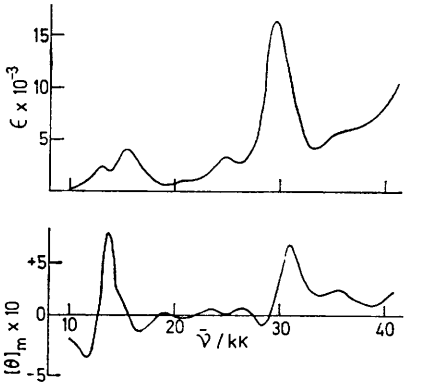

FIGURE 6 The absorption (upper curve) and m.c.d. (lower curve) spectra of $[Ta_6Cl_{12}]^{2+}$ in EtOH

The spectra of the complexes in the 2+ oxidation state were measured in ethanolic solution, and those of the oxidised complexes in ethanol saturated with HCl gas. The terminal ligand positions of the clusters were therefore solvated in the former case and substituted by chloride ion in the latter.[11] The results are generally in good agreement with those of Fleming and McCarley,[11] who also give tabulated spectra for clusters with a variety of terminal ligands. The following points should be noted.

(1) The close correspondence of bands below *ca.* 30,000 cm^{-1} in Figure 8 proves that they originate from metal–metal transitions. By analogy the bands below *ca.* 25,000 cm^{-1} in the niobium complexes are metal–metal bands. These are the bands which we seek to assign.

(2) There is a close correspondence of bands between niobium and tantalum clusters in the same oxidation state. The greatest differences occur in the lowest-energy bands of the 2+ and the 3+ oxidation states,

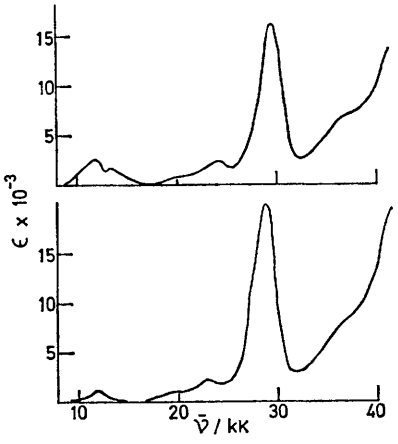

FIGURE 7 The absorption spectra of $[Ta_6Cl_{12}]^{3+}$ (upper curve) and $[Ta_6Cl_{12}]^{4+}$ (lower curve) in EtOH–HCl

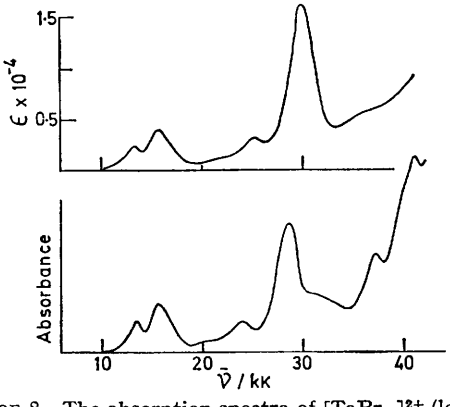

FIGURE 8 The absorption spectra of $[TaBr_{12}]^{2+}$ (lower curve) and $[Ta_6Cl_{12}]^{2+}$ (upper curve) in EtOH

there being an extra band in the tantalum complexes. The spectra of $(Nb_6Cl_{12})^{4+}$ and $(Ta_6Cl_{12})^{4+}$ are remarkably similar in all metal–metal bands, except for the report by Fleming and McCarley of a very weak band at 8600 cm^{-1} in the tantalum complex which is not evident in our spectra.

(3) The similarities in the spectra of Figures 3—5 and Figures 6—7 show that there can be no gross reordering of energy levels following oxidation.

(4) Two *A* terms of opposite sign appear under the lowest-energy bands of $(Ta_6Cl_{12})^{2+}$, but only one under the corresponding band of $(Nb_6Cl_{12})^{2+}$. Figures 9 and 10 show that these *A* terms disappear on oxidation.

(5) From Figure 10 it can be seen that considerable rotational strength is associated with the low-energy bands of the complex $(Ta_6Cl_{12})^{3+}$. The m.c.d. spectrum for the corresponding complex $(Nb_6Cl_{12})^{3+}$ could not be

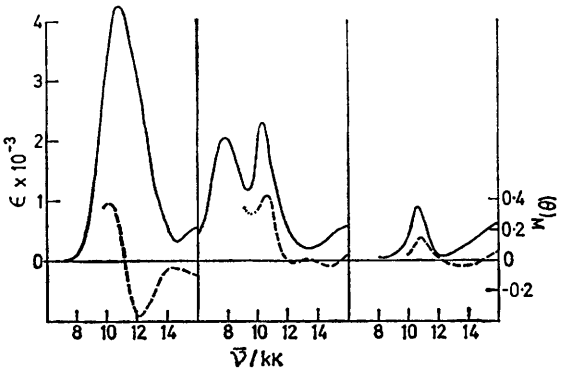

FIGURE 9 A comparison of the absorption (——) and m.c.d. (– – – –) spectra of the low-energy bands of $[Nb_6Cl_{12}]^{n+}$ where $n = 2$, 3, and 4 respectively

obtained below 10,000 cm^{-1}. Since the clusters in the 3+ oxidation state are paramagnetic with one unpaired spin,[10,18] the rather large rotational strength observed for these complexes may be the result of spin-dependent *C* term intensity. This is discussed in a later section.

(6) A positive *A* term is observed under the intense band at *ca.* 25,000 cm^{-1} in all three complexes $(Nb_6Cl_{12})^{n+}$ ($n = 2$, 3, or 4,) so that this transition is relatively unaffected by oxidation.

Schneider and Mackay [19] seek to explain the differences between the lowest-energy bands of $(Nb_6Cl_{12})^{2+}$ and $(Ta_6Cl_{12})^{2+}$ by postulating that the band envelope in the niobium complex covers two transitions. They claim some support for this from slight anomalies in the spectrophotometer trace. However we have measured the spectrum of $(Nb_6Cl_{12})^{2+}$ in a Perspex film at *ca.* 4 K, and while there is some sharpening of the bands there is no apparent splitting of the lowest energy band. Similarly there is no evidence of doubling in the solution m.c.d. spectrum (Figure 3).

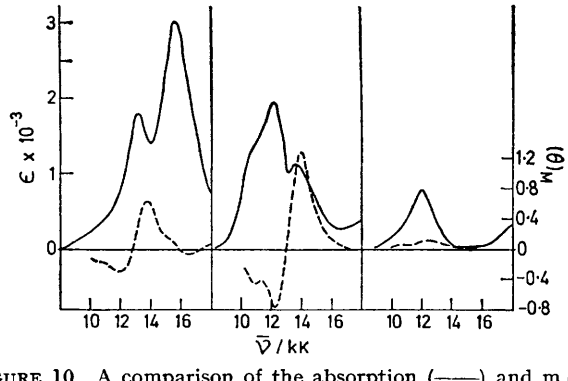

FIGURE 10 A comparison of the absorption (——) and m.c.d. (– – – –) spectra of the low-energy bands of $[Ta_6Cl_{12}]^{n+}$ where $n = 2$, 3, and 4 respectively

In the assignment of the cluster spectra we use only the signs of the *A* terms and not their absolute magnitudes. Nevertheless it is of interest to obtain some

estimate of the order of magnitude of the A terms as a check on the correctness of our various assumptions. This has been achieved for the lowest-energy bands of the clusters by a curve-fitting procedure according to equation (7), in which the line-shape functions f_1 and f_2 are assumed to be Gaussian in origin. Stephens [31] has recently pointed out that a moments analysis is a more rigorous method of extracting information from an m.c.d. spectrum when the bands are well resolved. However this is not the situation in the spectra of the niobium and tantalum cluster complexes, and since we are primarily interested only in the signs of the A terms we have not attempted a moments analysis. Using equation (7) and a value for the dipole strength from the approximate formula:

$$D = 0{\cdot}918 \times 10^{-2} \times \frac{\varepsilon_{max.} \times \nu_{\frac{1}{2}}}{\nu_{max.}} \text{ (debye)}^2 \quad (20)$$

the following results are obtained:

Cluster	Band maximum (cm^{-1})	A	A/D (β)
$(Nb_6Cl_{12})^{2+}$	10,800	$-3{\cdot}4$	$-0{\cdot}46$
$(Ta_6Cl_{12})^{2+}$	13,200	$+1{\cdot}3$	$+0{\cdot}43$
$(Ta_6Cl_{12})^{2+}$	15,600	$-0{\cdot}17$	$-0{\cdot}03$

Assignment of the Spectra.—Arguments based on the relative intensities of transitions have been used in previous attempts at the assignment of the cluster compound spectra.[3,11,19] Using simple MO theory it is easily shown [30] that transitions within a d-orbital subsystem are expected to be more intense than transitions between subsystems, although configuration interaction may cause intensity sharing. The simple model also suggests that the dipole length and hence the intensity of intra-subsystem transitions should increase with expansion of the cluster. Recent X-ray data shows that the niobium cluster expands on oxidation [11] and from Figures 3 and 5 it can be seen that the intense transition at *ca.* 25,000 cm^{-1} does, in fact, show a slight increase in intensity on oxidation. However, the corresponding band of the complex $(Nb_6Cl_{12})^{3+}$ (Figure 4) shows a reduction of peak height but an increase in width when compared with $(Nb_6Cl_{12})^{2+}$; this broadening of the band may be the result of spin-orbit coupling in the paramagnetic complex (*vide infra*).

It has been established (Appendix A) that the highest occupied orbital is spatially non-degenerate in both $(Nb_6X_{12})^{2+}$ and $(Ta_6X_{12})^{2+}$, and that the two-stage oxidation process corresponds to the removal of electrons from this orbital. Since the lowest-energy bands of both niobium and tantalum complexes show the largest changes on oxidation, these bands are assigned to transitions from the highest-occupied molecular orbital. From Figures 9 and 10 it can be seen that the major effects of oxidation on the low-energy bands are as follows.

(1) The dipole strength decreases. If these transitions originate from a non-degenerate orbital the dipole strength is expected to fall by a factor of 2 with the removal of one electron, and to be zero after two-electron oxidation.

(2) The number of bands increases by one following the removal of the first electron, and only one band with a weak shoulder remains after removal of the second electron. The extra band in the complexes $(M_6X_{12})^{3+}$ has been assigned to a transition into the hole left in the highest occupied MO [11,19] although the splitting could be the result of spin-orbit coupling. This is discussed in the following section.

Since the two oppositely-signed A terms under the lowest-energy bands of $(Ta_6Cl_{12})^{2+}$ disappear on oxidation we assign them to transitions from the highest occupied non-degenerate orbital. From the results of the MO calculation this orbital may have symmetry $a_{1g}(\theta)$ or $a_{2u}(\zeta)$. In both cases two symmetry-allowed transitions are possible, but from Table 4 it can be seen that only the transitions $a_{2u}(\zeta) \longrightarrow t_{2g}(\zeta)$ and $a_{2u}(\zeta) \longrightarrow t_{2g}(\xi,\eta)$ are predicted to show A terms of opposite sign. This assignment of the $a_{2u}(\zeta)$ orbital as the highest occupied MO agrees with the conclusions of Schneider and Mackay [19] but conflicts with those of Fleming and McCarley.[11] The latter authors preferred the $a_{1g}(\theta)$ orbital as the highest-occupied since they report that the bonds between metal atoms and terminal ligands shorten on oxidation, and this appears more consistent with the removal of electron density from the metal d_{z^2} orbitals. However, we feel our assignment to be based on less equivocal facts, and to be more compatible with MO energy considerations (see below).

If this conclusion is accepted, the $t_{2g}(\xi,\eta)$ orbital cannot be occupied in the ground state as predicted by Cotton and Haas. However, in order to accommodate the 16-valence electrons satisfactorily it must be substituted by another triply-degenerate orbital. As discussed earlier we now incorporate both the metal–halogen interaction and the energy-level diagrams shown in Figure 2 into a theoretical bonding scheme compatible with the experimental results. It should be noted that this scheme maintains the relative ordering of MO's derived from each d-orbital subsystem obtained from the Hückel calculation, and lifts the degeneracy of the subsystems according to equation (1). It is therefore by no means entirely arbitrary. The scheme is represented diagrammatically in Figure 11, where only the gross ordering of levels is suggested, the energy spacings not being significant. Indeed, the bracketed orbitals may be sufficiently close in energy that electron repulsion terms decide the ordering of excited states of the system. Similarly there may be appreciable mixing of MO's of like symmetry since the energy gaps between them may not be large.

In some ways, however, this choice of bonding orbitals is unfortunate. Using a topological approach Kettle [4] has shown that the bonding MO's in the octahedral cluster compounds can be associated with the 8 faces and 12 edges of the octahedron. In the complexes $(M_6X_{12})^{2+}$

[31] P. J. Stephens, *J. Chem. Phys.*, 1970, **52**, 3489.

the metal–metal bonding orbitals are associated with the octahedron faces and the metal–halogen orbitals with the edges, and *vice versa* for the complex $(Mo_6X_8)^{4+}$. The 8 faces of the octahedron generate the representation $A_{1g} + A_{2u} + T_{1u} + T_{2g}$ of the 0_h group, which corresponds with the symmetries of the metal–metal bonding orbitals for $(M_6X_{12})^{2+}$ predicted by Cotton and Haas. This agreement does not occur with our assignment, and the physical principles possibly underlying this discrepancy are discussed with reference to a crystal-field model in a later section.

Using the signs of the observed A terms and the energy-level diagram of Figure 11 the transition at 13,200 cm^{-1} in the spectrum of $(Ta_6Cl_{12})^{2+}$ is assigned to $a_{2u}(\zeta) \longrightarrow t_{2g}(\zeta)$, and that at 15,600 cm^{-1} to $a_{2u}(\zeta) \longrightarrow t_{2g}(\xi,\eta)$. The intense band at *ca.* 25,000 cm^{-1} in the niobium complexes and *ca.* 30,000 cm^{-1} in the tantalum

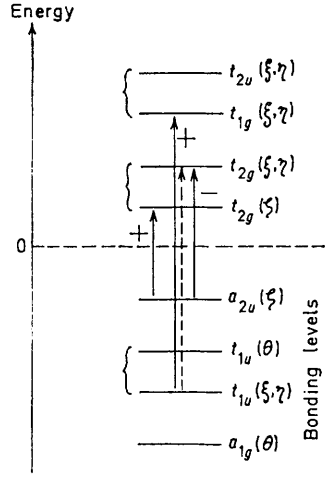

FIGURE 11 An energy-level diagram derived from the assignment of the m.c.d. spectra of the tantalum clusters. Transitions assigned in this work and the signs of their associated A terms are indicated

complexes is assigned to the transition $t_{1u}(\xi,\eta) \longrightarrow t_{1g}(\xi,\eta)$. This is consistent with the observed positive A term (Table 4), with the high intensity characteristic of an intra-subsystem transition, and with the fact that it is relatively unaffected by oxidation.

However the transition $t_{1u}(\zeta,\eta) \longrightarrow t_{2g}(\xi,\eta)$ is expected to occur at lower energy than $t_{1u}(\xi,\eta) \longrightarrow t_{1g}(\xi,\eta)$, and since Table 4 shows the sign of the A term for the former transition to be uncertain there remains an ambiguity in the assignment of the intense d–d band. On the other hand only these two possible assignments satisfy all the experimental criteria.

It must be admitted, however, that there are anomalies in this scheme. First, the positive A term under the lowest-energy band of $(Ta_6Cl_{12})^{2+}$ originates from the transition $a_{2u}(\zeta) \longrightarrow t_{2g}(\zeta)$, and according to the simple model should be associated with the more intense of the two low-energy bands since it is an intra-subsystem transition. The fact that this is not the case may be the result of mixing between the orbitals $t_{2g}(\zeta)$ and $t_{2g}(\xi,\eta)$. Secondly, the scheme offers no simple explanation of the differences between the niobium and tantalum complexes, although it should be remembered that the calculation applies specifically to the tantalum complex alone. Robin and Kuebler [3] have suggested that the apparent doubling of the low-energy band of $(Ta_6Cl_{12})^{2+}$ is caused by tetragonal distortion of the octahedral complex. The two observed bands are then assigned to excited states of A and E symmetry, but this conclusion is not consistent with the m.c.d. spectrum (Figure 6) since the A terms associated with the low-energy bands indicate that both transitions involve orbitally degenerate excited states.

Spin-orbit Coupling.—It is now possible to test these assignments by prediction of spin-orbit coupling effects in the absorption spectra of the cluster $(M_6X_{12})^{n+}$, and of C terms in the m.c.d. spectra of the complexes $(M_6X_{12})^{3+}$. Because the electric dipole moment operator $\hat{m}$ is independent of spin, C terms will only be present in the spectra if spin-orbit coupling is appreciable.[32]

Spin-orbit coupling may be introduced into the calculation in two different ways. First we may use a Russell–Saunders scheme in which transitions occur between terms that may be split by the spin-orbit interaction. Clearly if the ground state of the system is a spin singlet then in first-order electric-dipole allowed transitions in the Russell–Saunders scheme will not be split by spin-orbit coupling. Alternatively we may use an intermediate coupling scheme in which the orbital and spin angular momenta of individual electrons in each subsystem couple strongly. Spin-orbit coupling terms in the Hamiltonian are then much larger than electron repulsion terms, but still smaller than the metal–metal and metal–halogen interactions, and transitions are considered to occur between the resulting one-electron spinor orbitals. This type of scheme has been used successfully by Jørgensen in the interpretation of the charge-transfer spectra of hexahalide complexes of third-row transition elements,[33] and is attractive in the present context since it offers a possible explanation of the otherwise puzzling differences between the lowest-energy bands of the complexes $(Nb_6Cl_{12})^{2+}$ and $(Ta_6Cl_{12})^{2+}$. However a more detailed consideration of the scheme, given in Appendix B, shows that its predictions do not agree with experimental fact. On the other hand agreement between theory and experiment is very good if Russell–Saunders coupling is used, and we therefore concentrate on this scheme in the following discussion.

In the Russell–Saunders scheme spin-orbit coupling is only significant in first order for the clusters $(M_6X_{12})^{3+}$, since the 2+ and 4+ oxidation states have $^1A_{1g}$ ground states and only singlet states are electric-dipole allowed. In the postulated bonding scheme allowed transitions will be $^2A_{2u} \rightarrow {}^2T_{2g}$, and under the influence of spin-orbit coupling a $^2T_{2g}$ state may split into E_g'' and U_g'

[32] M. J. Harding, S. F. Mason, D. J. Robbins, and A. J. Thomson, *J. Chem. Soc.* (*A*), 1971, 3047.
[33] C. K. Jørgensen, *Mol. Phys.*, 1959, **2**, 309.

components.[21a] Using Griffith's formalism [28] the energies of these components are found to be:

$$W(E'') = \tfrac{1}{3}\langle {}^2T_2||\Sigma\hat{s}\,.\,\hat{u}||{}^2T_2\rangle$$
$$W(U') = -\tfrac{1}{6}\langle {}^2T_2||\Sigma\hat{s}\,.\,\hat{u}||{}^2T_2\rangle \qquad (21)$$

where $\Sigma\hat{s}\,.\,\hat{u}$ is the spin-orbit coupling operator for the system. Here $\hat{u} = \zeta_d\,.\,\hat{\mathbf{l}}$.

Consider first the one-electron excitation $a_{2u} \longrightarrow t_{2g}$. For the ${}^2T_{2g}$ excited state we have: [29]

$$\langle (t_2{}^1){}^2T_2||\Sigma\hat{s}\,.\,\hat{u}||(t_2{}^1){}^2T_2\rangle = i\frac{\sqrt{6}}{2}\langle t_2||\zeta_d\,.\,\hat{\mathbf{l}}||t_2\rangle \qquad (22)$$

We next assume that in the evaluation of the spin-orbit matrix elements from the LCAO–MO's it is only necessary to retain one-centre angular momentum integrals, since the parameter $\zeta_d(r)$ varies inversely as the cube of the electron-nuclear separation and effectively weights the region close to the nucleus. It is then evident that in first order spin-orbit coupling will be quenched in all the

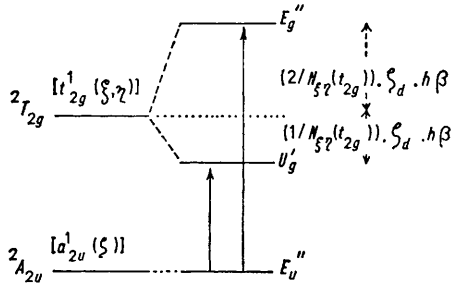

FIGURE 12 Spin-orbit splitting of the ${}^2T_{2g}[t_{2g}{}^1(\xi,\eta)]$ state in the $(Ta_6Cl_{12})^{3+}$ complex. Allowed transitions are indicated

d-orbital subsystems except $|d_{yz},d_{zx}|$. Hence with one-centre orbital angular momentum matrix elements derived from Table 3 we have:

$$\langle (t_2{}^1){}^2T_2||\Sigma\hat{s}\,.\,\hat{u}||(t_2{}^1){}^2T_2\rangle$$
$$= \frac{6}{N_{\xi\eta}(t_{2g})}\,.\,\zeta_d\,.\,\hbar\beta \text{ when } t_2 = t_{2g}(\xi,\eta) \qquad (23)$$
$$= 0 \text{ when } t_2 = t_{2g}(\zeta)$$

Therefore in first order the transition $a_{2u}(\zeta) \longrightarrow t_{2g}(\zeta)$ is unaffected by spin-orbit coupling and should be unchanged on oxidation from $(M_6X_{12})^{2+}$ to $(M_6X_{12})^{3+}$. However the transition $a_{2u}(\zeta) \longrightarrow t_{2g}(\xi,\eta)$ should split into two components in the oxidised cluster, as shown in Figure 12. The lower-energy component is predicted to be twice as intense as the higher energy one.

The C terms associated with the spin-orbit components are found to be:

$$C[E_u''({}^2A_{2u}) \longrightarrow E_g''({}^2T_{2g})] = -\tfrac{1}{3}\beta|M'|^2$$
$$C[E_u''({}^2A_{2u}) \longrightarrow U_g'({}^2T_{2g})] = +\tfrac{1}{3}\beta|M'|^2 \qquad (24)$$
$$\text{where } M' = \langle {}^2A_{2u}||\hat{m}||{}^2T_{2g}\rangle$$

Because of the negative sign appearing in equation (7) the spin-orbit components E'' and U' derived from the $t_{2g}{}^1(\xi,\eta)$ configuration should be associated with positive and negative dichroism respectively. The spectra shown in Figure 10 confirm these predictions for $(Ta_6Cl_{12})^{3+}$, as discussed below.

The band at 13,200 cm^{-1} in $(Ta_6Cl_{12})^{2+}$ is assigned to the transition $a_{2u}(\zeta) \longrightarrow t_{2g}(\zeta)$. On oxidation it should remain unsplit, but reduced in magnitude by a factor $\frac{1}{2}$. We therefore assign the shoulder at 10,600 cm^{-1} to this transition. The band at 15,600 cm^{-1} in $(Ta_6Cl_{12})^{2+}$ is assigned as $a_{2u}(\zeta) \longrightarrow t_{2g}(\xi,\eta)$, and we propose that this band splits in $(Ta_6Cl_{12})^{3+}$ to give bands at 12,150 and 13,600 cm^{-1} arising from the U' and E'' spin-orbit components of the ${}^2T_{2g}[t_{2g}{}^1(\zeta,\eta)]$ state. This assignment is then consistent with the following facts. (i) The decrease in absolute intensity by a factor *ca.* $\frac{1}{2}$ on oxidation. (ii) The intensity ratio of *ca.* 2 : 1 for the U' and E'' components. (iii) The splitting of the spin-orbit components by *ca.* 1500 cm^{-1} measured from peak maxima. Neglecting overlap in normalisation the predicted splitting is $\frac{3}{4}\zeta_d\,.\,\hbar\beta$, in reasonable agreement with the observed value since $(\zeta_d\,.\,\hbar\beta)$ is 1657 cm^{-1} for the tantalum atom [21] and will be higher for the ion in formal oxidation state $+2\frac{1}{2}$. (iv) The large negative and positive dichroism associated respectively with the U' and E'' components. We therefore ascribe this large rotational strength to spin-dependent C term intensity. However temperature dependence studies are required to obtain the magnitude of these C terms and produce final confirmation of the assignment.

We next consider the intense band at *ca.* 25,000 cm^{-1} in $(Nb_6Cl_{12})^{n+}$ and *ca.* 30,000 cm^{-1} in $(Ta_6Cl_{12})^{n+}$, which we have assigned to one of the transitions $t_{1u}(\xi,\eta) \longrightarrow t_{1g}(\xi,\eta)$ or $t_{1u}(\xi,\eta) \longrightarrow t_{2g}(\xi,\eta)$. This transition is complicated by the fact that the excited state ${}^2T_{2g}(a_{2u}{}^1t_{1u}{}^5t_{jg}{}^1)$ ($j = 1$ or 2) comprises three open shells. The orbital product $(a_{2u} \times t_{1u} \times t_{1g})$ gives the sum $A_{2g} + E_g + T_{1g} + T_{2g}$, and there is no ambiguity in the coupling since no representation occurs more than once. [A similar result follows for the $t_{2g}(\xi,\eta)$ orbital.] However the three spins may couple to produce two independent sets of doublets and a set of quartet states. If the α-spin component of the ground state of the system is denoted in determinantal form by: $|at_u\bar{t}_u\rangle$ (where the bar implies β-spin) then the corresponding α-spin components of the excited state doublet wavefunctions will be linear combinations of the three determinants: $|at_u\bar{t}_g\rangle$; $|a\bar{t}_ut_g\rangle$; $|\bar{a}t_ut_g\rangle$.

Using the following linear combinations:

(i) $1/\sqrt{6}[2|\bar{a}t_ut_g\rangle - |at_u\bar{t}_g\rangle - |a\bar{t}_ut_g\rangle]$
(ii) $1/\sqrt{2}[|at_u\bar{t}_g\rangle - |a\bar{t}_ut_g\rangle]$

it is found that the ground-state spin wavefunction is orthogonal to (i) but not to (ii). Hence the electric-dipole allowed transition occurs to the ${}^2T_{2g}$ state in which the electron in the a_{2u} orbital is unaffected, and is in fact coupled to the singlet state ${}^1T_{1u}$ of the configuration $(t_{1u}{}^5t_{jg}{}^1)$. Using the method outlined earlier in this section it is now possible to calculate the matrix element

of spin-orbit coupling analogous to equation (23). This is found to be:

$$\langle a_{2u}{}^1(^2A_{2u})t_{1u}{}^1t_{1g}{}^1(^1T_{1u})^2T_{2g}\|\Sigma\hat{s}\cdot\hat{u}\|a_{2u}{}^1(^2A_{2u})\text{-}\\ t_{1u}{}^1t_{1g}{}^1(^1T_{1u})^2T_{2g}\rangle = 0 \quad (25)$$

Hence although spin-orbit coupling is not quenched within the $|d_{yz},d_{zx}|$ subsystem the intense band is not split in first order. Essentially this arises because the one-electron excitation involved is independent of the unpaired electron in the a_{2u} orbital, and the same result holds for transitions $t_{1u} \longrightarrow t_{1g}$ and $t_{1u} \longrightarrow t_{2g}$. Both possible assignments for the intense band are therefore consistent with the experimental observation that this band does not split on oxidation, and that in this region of the spectrum the m.c.d. shows no change attributable to C term intensity. The very slight broadening of the intense band in $(Nb_6Cl_{12})^{3+}$ which was mentioned earlier may be the result of second-order spin-orbit effects.

The assignments made on the basis of the observed A terms in the spectra of the $(M_6X_{12})^{2+}$ clusters are therefore substantiated by consideration of spin-orbit effects. The lowest-energy bands of the species $(M_6X_{12})^{4+}$ have been assigned to transitions into the vacant $a_{2u}(\zeta)$ orbital, but they may be present and simply masked by more intense bands in the spectra of complexes in lower oxidation states. With the bonding scheme of Figure 11 there can be no electric-dipole allowed transitions into the $a_{2u}(\zeta)$ orbital, although such transitions might gain intensity by a vibronic mechanism.

An Alternative Theoretical Model.—It has been pointed out in the earlier discussion that our assignment of metal–metal bonding orbitals is not consistent with the topological approach adopted by Kettle. The symmetries of these bonding orbitals in the two cases are predicted to be:

$$a_{1g} + a_{2u} + t_{1u} + t_{2g} \quad \text{Kettle}^4$$
$$a_{1g} + a_{2u} + t_{1u} + t_{1u} \quad \text{this work}$$

However to some extent it is possible to justify our assignment from consideration of a third theoretical model, *viz.* that of the crystal field. This model has been applied to polyhedral boron hydrides by Hoffmann and Gouterman,[34] and we draw largely on their results which apply quite generally to large cluster complexes.

In essence the model considers each electron to move in a one-electron field created by some parametric effective charge at each nucleus. The Coulomb interaction between each electron and the complete set of nuclei is expanded in a series of spherical harmonic terms,[35] and zeroth-order wavefunctions are obtained by solving the one-electron Hamiltonian with only the first, spherically symmetric term in the crystal-field expansion being retained. The energy levels, in order of increasing energy, are found to be: $1s,2p(2s,3d)(3p,4f)\ldots$ where approximately degenerate levels are in parentheses and conventional spectroscopic notation for principal and azimuthal quantum numbers n, l is used. As a second step the higher-order spherical harmonic terms in the crystal-field potential are included as a perturbation. This is only carried out qualitatively, however, since for values of $l > 3$ the ordering of levels depends on more than one perturbing crystal-field term. Finally, Hoffmann and Gouterman show that if the electron is restricted within a spherical shell containing the nuclei, the orbitals involving radial nodes are raised in energy. Since this is perhaps a more realistic approximation we shall consider only nodeless orbitals when seeking the lowest-energy bonding orbitals, *i.e.* $1s,2p,3d,4f\ldots$ It is now necessary to estimate qualitatively the interaction of each electron with the crystal field, and to do this it must be realised that there are two fields of opposite sign within each cluster complex. There is first the stabilising interaction with the nuclei of the metal atoms situated along the axes of the octahedron, and secondly the destabilising interaction with the electron density of the bridging halogen atoms situated above the octahedron edges. The situation is summarised in Table 5, the columns of which

TABLE 5

Comparison of the crystal field and LCAO models

1	2	3	4	5	6	7
$1s$	a_{1g}	1	(θ)	Totally symmetric		
$2p$	t_{1u}	x	(θ)	Axial density	−	−
$3d$	e_g	(x^2-y^2)	(θ)	Axial density		
	t_{2g}	xy	(ξ,η)	Axial nodes, density weighted to edges	+	+
$4f$	a_{2u}	xyz	(ζ)	Axial nodes, density weighted to faces		
	t_{2u}	$z(x^2-y^2)$	(ξ,η)	Axial nodes, density weighted to edges	−	+
	t_{1u}	$z(5z^2-3r^2)$	(ξ,η)	Density principally along z-axis	+	−

give the following information: (1) the zeroth-order crystal-field levels; (2) the levels in the octahedral crystal field (order not significant); (3) a representative function forming a basis for the appropriate irreducible representation of the group O_h;[35] (4) the LCAO subsystem from the calculation in this work which gives an orbital most closely reproducing the electron distribution of the crystal-field orbital; (5) a brief summary of the distribution of electron density in the crystal field. The spatial distribution of f-orbitals is given pictorially by Friedman *et al.*;[36] (6) the sign of the reduced magnetic moment matrix element for the crystal-field orbital;[28] (7) as (6) for the corresponding LCAO orbital.

From the Table it can be seen that the $t_{2g}(3d)$ crystal-field orbital places electron density along the octahedron edges, thereby suffering maximum destabilisation by interaction with the bridging halogen atoms. The overlap regions of the $t_{2g}(\xi,\eta)$ molecular orbital produce a similar electron distribution, and it is perhaps not

[34] R. Hoffman and M. Gouterman, *J. Chem. Phys.*, 1962, **36**, 2189.

[35] C. J. Ballhausen, 'Introduction to Ligand Field Theory,' McGraw-Hill Book Company, New York, 1962.

[36] H. G. Friedman, G. R. Choppin, and D. G. Feuerbacher, *J. Chem. Ed.*, 1964, **41**, 354.

surprising that our experimental results lead to the conclusion that this orbital is not occupied in the ground state, in contrast to the predictions of Cotton and Haas and of Kettle. In fact it can be seen from Table 5 that the bonding orbitals assumed in this work produce electron distributions equivalent to crystal-field orbitals which concentrate electron density either along the axes or on the faces of the octahedron, thereby maximising interactions with the metal nuclei and minimising interaction with the bridging halogen atoms.

It should be noted however that in some cases the predictions of the LCAO scheme and of the crystal-field model are quite different. For example, the $e_g(3d)$ orbital in the latter case is stabilised by strong interaction with the metal nuclei, but the equivalent $e_g(\theta)$ orbital in the LCAO scheme is destabilised because of considerable negative overlap [34] (Figure 2). Since there is evidently some truth in both these approximations the relative energy of this orbital cannot be predicted easily. Secondly, Table 5 shows that the two schemes may predict different angular momenta for equivalent orbitals.

In this connection it is of interest to note that a model involving delocalised electrons restricted to a spherical shell containing the nuclei, which has previously been used to describe the *F* centre in alkali-halide crystals,[37] has also been applied in this laboratory to these cluster complexes.[38] This model has successfully predicted the observed transition energies but has not so far proved capable of reproducing the m.c.d. spectrum.

SUMMARY

The observation of *A* terms in the m.c.d. spectra of the cluster compounds $(M_6X_{12})^{2+}$ has allowed the assignment of several of their electronic transitions. These assignments are confirmed by consideration of spin-orbit coupling effects in the spectra of the oxidised complexes. The theoretical model used to interpret the spectra includes both metal–metal and metal–ligand interactions, with spin-orbit coupling introduced in a Russell–Saunders scheme as a final perturbation. The spectral bands are assigned to pure one-electron transitions, and hence although electron-repulsion terms appear sufficiently large to make Russell–Saunders coupling appropriate for these compounds they are not so large that the spectra become complicated by extensive configuration interaction. The bonding scheme consistent with our assignments does not agree with the predictions of Cotton and Haas [2] or of Kettle,[4] but appears to be supported by consideration of the effective crystal field within each cluster complex.

Finally, it has been assumed that these transitions assigned in this work are electric-dipole allowed, and in view of their intensity this assumption seems reasonable. Temperature-dependence studies should confirm this, and also provide magnitudes for the *C* terms predicted in the spectra of the $(M_6X_{12})^{3+}$ complexes.

EXPERIMENTAL

Materials.—$Nb_6Cl_{14}.8H_2O$ was prepared from niobium by heating the latter in chlorine to give $NbCl_5$.[39] The pentachloride was reduced with cadmium filings and extracted with hot acid. The tantalum chloride was prepared as the anhydrous solid Ta_6Cl_{15} using a modification of the method given by Kuhn and McCarley.[40] Tantalum was heated first in a stream of nitrogen to dry it thoroughly and then at 400 °C in chlorine gas. The resulting $TaCl_5$ was reduced with aluminium foil formed into small rolls which had been dried in an oven. The reduction was carried out in a sealed, evacuated tube inclined at an angle with a temperature gradient of 400—250 °C maintained along the tube for 36 h to create a reflux action. Ta_6Cl_{15} was obtained in good yield in this way. In the case of the bromides, the pentabromide was first prepared by carrying a stream of very dry bromine with nitrogen over the hot metal.

Spectra were run in solution and in most cases the appropriate oxidation state was generated in solution from stock solutions of the solid compounds in absolute alcohol. Particular care is needed with the tantalum complexes to avoid mixtures of oxidation states.[12] $[Nb_6Cl_{12}]^{2+}$ and $[Ta_6Cl_{12}]^{2+}$ were prepared by allowing a stock solution to stand over amalgamated zinc and a stream of nitrogen saturated with solvent was bubbled through. Portions of the solution were transferred to the measuring cell by syringe under nitrogen.

$[Nb_6Cl_{12}]^{3+}$ was prepared from a stock solution saturated with HCl gas, oxidised by a stream of oxygen, and resaturated with HCl. $[Nb_6Cl_{12}]^{4+}$ and $[Ta_6Cl_{12}]^{4+}$ were prepared in the same manner but with chlorine as the oxidant. $[Ta_6Cl_{12}]^{3+}$ was obtained by chlorine oxidation of acidified $[Ta_6Cl_{12}]^{2+}$ to the point at which the intense absorption at 15,600 cm^{-1} disappeared. Good agreement was obtained with the spectra of the tetraethylammonium salts of the totally anated ions.[12,40]

In acid solutions the complexes are totally anated with the exception that it is not possible to prepare the ions $[(M_6X_{12})X_6]^{4-}$ in this manner because mixtures of oxidation states result.[12] On the other hand solutions of complexes in 3+ and 4+ oxidation states must remain saturated with HCl to prevent mixtures of oxidation states being formed. The oxidation can be reversed by adding zinc.

All solutions were freshly prepared before measurement of their spectra. Following the measurement of m.c.d. the absorption spectra of the samples used were checked to ensure that there had been no change in oxidation state.

Instruments.—Absorption spectra were measured with a Cary 14 spectrophotometer. M.c.d. spectra were measured on three circular dichrographs by means of a superconducting solenoid (Oxford Instrument Co.). The samples were held at room temperature in a field of 48 kgauss over a 1-cm path length. The dichrographs were the Jouan Mark II (range 610—185 nm), Cary 61 (range 610—185 nm), and a dichrograph built in this laboratory with a useful range 1000—500 nm.[41,42]

[37] T. F. Hunter, *Mol. Phys.*, 1968, **14**, 171.
[38] H. Cartwright, R. Grinter, and T. F. Hunter, unpublished results.
[39] H. S. Harned, L. Pauling, and R. B. Corey, *J. Amer. Chem. Soc.*, 1960, **82**, 4815.
[40] P. J. Kuhn and R. E. McCarley, *Inorg. Chem.*, 1965, **4**, 1482.
[41] R. Grinter, M. J. Harding, and S. F. Mason, *J. Chem. Soc.* (*A*), 1970, 667.
[42] B. R. Hollebone, S. F. Mason, and A. J. Thomson, *Symp. Faraday Soc.*, 1969, **3**, 146.

APPENDIX A

A central assumption in our interpretation of the cluster compound spectra is that the highest-occupied orbital is non-degenerate. This is entirely consistent with magnetic susceptibility and e.p.r. data,[10,18] but it is necessary to demonstrate that these data are inconsistent with a degenerate orbital lying highest.

All shells are assumed filled in the ground state of the species $(M_6X_{12})^{2+}$. The highest-occupied orbital cannot be of e symmetry since two-electron oxidation would leave a paramagnetic ground state, in contrast to the observed diamagnetism of the species $(M_6X_{12})^{4+}$. However if the orbital were of t_1 or t_2 symmetry the configuration t^4 can give the terms $^3T_1$, $^1A_1$, ^1E, $^1T_2$, and if the triplet term were to be lowest it could be split by spin-orbit coupling to give the components A_1, E, T_1, T_2 in the 0_h double group. It is thus possible for a state of zero angular momentum to form the ground state of the system.

In order to discount this possibility, consider first the one-electron oxidation to $(M_6X_{12})^{3+}$. The observed g-values are close to the free-electron value for these complexes,[10,18] and μ_{eff} is near the spin-only value for one unpaired electron.[18] The terms $^2T_j(t_j^5)$ [where $j = 1$ or 2] should produce an appreciable orbital contribution to the magnetic moment, in disagreement with the experimental data. If spin-orbit coupling is appreciable the g-values of the resulting spin-orbit states are:

$$E'(^2T_1) \text{ or } E''(^2T_2) \quad g = \left[\frac{2}{3} + \frac{4i}{3\sqrt{6}}\langle t_j\|1\|t_j\rangle\right]$$
$$U'(^2T_j) \quad g = \left[\frac{2}{3} - \frac{2i}{3\sqrt{6}}\langle t_j\|1\|t_j\rangle\right] \qquad \text{(A1)}$$

It would clearly be fortuitous if the g-values for these states were to reproduce the free-electron value, and this is certainly not the case with the angular momenta derived from Table 3. Similarly the effective magnetic moment from the formula $\mu_{eff} = g\sqrt{J(J+1)}$ is not expected to mimic the spin-only value for one unpaired electron.

Secondly it is clear that if spin-orbit coupling were important in determining the ground state of the oxidised clusters $(M_6X_{12})^{n+}$ ($n = 3$ or 4) there should be several states lying close in energy to the ground state, giving rise to the following experimental features. (i) Temperature-independent paramagnetism (TIP) in the niobium clusters very much larger than in corresponding tantalum clusters, since ζ_d is much smaller in the former. Although TIP is larger in the niobium clusters [18] this is only by a relatively small amount, and is probably explained by the lower energy of spectral bands in the near-i.r. and visible for the niobium complexes.

(ii) TIP for the species $(M_6X_{12})^{n+}$ ($n = 3$ or 4) should be much larger than for $(M_6X_{12})^{2+}$. This is not the case.[18] Hence the non-degeneracy of the highest occupied orbital in these clusters seems well established.

APPENDIX B

At first sight it seems possible that use of the intermediate coupling scheme for the spin-orbit interaction could explain the differences in the lowest-energy bands of $(Ta_6Cl_{12})^{2+}$ and $(Nb_6Cl_{12})^{2+}$. Here we wish to show that this is not the case.

Using the results of Appendix A and the fact that the lowest-energy bands disappear following two-electron oxidation, the assignment of these bands to transitions from the $a_{2u}(\zeta)$ or $a_{1g}(\theta)$ orbitals is well established. Since spin-orbit coupling is assumed quenched by the ligand field in all subsystems except $|d_{xz},d_{xx}|$ we consider only the two possible electric-dipole allowed transitions $a_{1g}(\theta) \longrightarrow t_{1u}(\xi\eta)$ and $a_{2u}(\zeta) \longrightarrow t_{2g}(\xi\eta)$ as those which may give rise to the lowest-energy bands. Take first $a_{1g} \longrightarrow t_{1u}$. The coupling of orbital and spin angular momenta for the individual electrons gives spinor orbitals with the following symmetries in the 0_h double group:

$$a_{1g} \times E' \longrightarrow e'_g$$
$$t_{1u} \times E' \longrightarrow e'_u + u'_u \qquad \text{(B1)}$$

The ground state is A_{1g} in $(M_6X_{12})^{2+}$. For each possible transition the excited states are:

$$e'_g \longrightarrow e'_u\colon\ A_{1u} + T_{1u}$$
$$e'_g \longrightarrow u'_u\colon\ E_u + T_{1u} + T_{2u} \qquad \text{(B2)}$$

Electric-dipole transitions are allowed to the T_{1u} states. One way to calculate the energies, intensities and A terms for these transitions is to use appropriate Russell–Saunders states as a basis set in which to diagonalise the spin-orbit coupling operator. For example the transition $a_{1u} \longrightarrow t_{1u}$ gives $^1T_{1u}$ and $^3T_{1u}$ excited states, which are now considered degenerate in the absence of spin-orbit coupling, and we use the T_{1u} spin-orbit components from the singlet and triplet terms to construct the secular determinant for the spin-orbit coupling energies of the electric-dipole allowed states in intermediate coupling. Retaining only one-centre angular momentum integrals as before we find:

$$\begin{vmatrix} ^1T_1(T_1) & ^3T_1(T_1) \\ (O-E) & \frac{\sqrt{2}\zeta}{N_{\xi\eta}(t_{1u})} \\ \frac{\sqrt{2}\zeta}{N_{\xi\eta}(t_{1u})} & \left(-\frac{\zeta}{N_{\xi\eta}(t_{1u})} - E\right) \end{vmatrix} = 0 \qquad \text{(B3)}$$

The eigenvalues and eigenvectors are:

$$E = -\frac{2\zeta}{N_{\xi\eta}(t_{1u})} : |T_1\rangle = \frac{1}{\sqrt{3}}|^1T_1(T_1)\rangle - \frac{\sqrt{2}}{\sqrt{3}}|^3T_1(T_1)\rangle$$
$$E = +\frac{\zeta}{N_{\xi\eta}(t_{1u})} : |T_1'\rangle = \frac{\sqrt{2}}{\sqrt{3}}|^1T_1(T_1)\rangle + \frac{1}{\sqrt{3}}|^3T_1(T_1)\rangle \qquad \text{(B4)}$$

The intensities of transitions to these states are given by the square of the coefficient for the $^1T_1$ term, and clearly the lower-energy transition is predicted to have half the intensity of the higher-energy one. From Figure 10 it can be seen that just such an effect occurs in the low-energy bands of $(Ta_6Cl_{12})^{2+}$; it could then be said that the corresponding band in $(Nb_6Cl_{12})^{2+}$ is unsplit because ζ_d is very much smaller. However it is straight-forward to show that the eigenvectors of equation (B4) predict A terms of the same sign for the states $|T_1\rangle$ and $|T_1'\rangle$, and this does not agree with the m.c.d. spectrum in Figure 10.

If we next consider the transition $a_{2u}(\zeta) \longrightarrow t_{2g}(\xi\eta)$ a similar treatment to that above shows that the lower energy of the two transitions is predicted to be the more intense, which is again in contrast to experimental fact for $(Ta_6Cl_{12})^{2+}$. The Russell–Saunders scheme gives much better qualitative

agreement with the observed spectra, and is therefore to be preferred over the intermediate coupling scheme. The close correspondence between the spectra of the niobium and tantalum clusters would also argue that spin-orbit coupling is not dominant in determining the one-electron energy levels, since the parameter ζ_d is markedly different in the two cases.

We thank the S.R.C. for a Research Studentship (D. J. R.) and for the provision of c.d. spectrophotometers, and Professor S. F. Mason for making equipment available, also Dr. R. Grinter and Mr. H. Cartwright for discussions and help with computing. Useful discussions with Dr. P. Day and Mr. P. A. Cox on the consequences of spin-orbit coupling are gratefully acknowledged. Finally we thank Mr. M. W. Bee and Mr. J. T. Arkley, Third Year Undergraduates at the University of East Anglia, for preparation of some of the materials used in this work.

[2/371 *Received*, 18*th February*, 1972]